The Journal of Physical Chemistry Letters

Letter

pubs.acs.org/JPCL

Surface Isotope Segregation as a Probe of Temperature in Water Nanoclusters

Pablo E. Videla,[†] Peter J. Rossky,[‡] and Daniel Laria*[,†,§]

[†]Departamento de Química Inorgánica Analítica y Química−Física e INQUIMAE, Facultad de Ciencias Exactas y Naturales, Universidad de Buenos Aires, Ciudad Universitaria, Pabellón II, 1428 Buenos Aires, Argentina

[‡]Department of Chemistry, The University of Texas at Austin, Austin, Texas 78712-0165, United States

[§]Departamento de Física de la Materia Condensada, Comisión Nacional de Energía Atómica, Avenida Libertador 8250, 1429 Buenos Aires, Argentina

Supporting Information

ABSTRACT: Using ring polymer molecular dynamics simulations, we examine equilibrium and dynamical characteristics of solid-like, aqueous clusters that combine isotopic mixtures of HDO dilute in H_2O, at temperatures intermediate between 50 and 175 K. In particular, we focus attention on the relative thermodynamic stabilities of the two isotopes at dangling hydrogen bond sites. The water octamer is analyzed as a reference system. For this aggregate, decreasing temperature yields a gradual stabilization of the light isotope at dangling sites in molecules acting as single-donor-double-acceptors of hydrogen bonds. At $T \sim 50$ K, the imbalance between the corresponding quantum kinetic energies leads to a free energy difference between dangling and hydrogen bonded sites of the order of $\sim 2k_BT$. Similar free energy differences were found at dangling sites in $N_w = 50$ water clusters. The extent of the H/D segregation can be adequately monitored by modifications in the peak intensity of the high frequency shoulder of the stretching band of the infrared spectrum. These signals, in turn, represent a potential experimental signature of the elusive temperature of clusters in molecular beams.

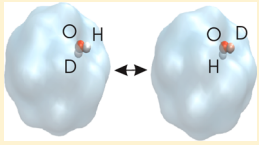

SECTION: Liquids; Chemical and Dynamical Processes in Solution

The recent advent of surface-sensitive spectroscopic techniques performed at water/air interfaces[1−4] has clearly revealed the presence of a sharp peak in the vicinity of the free O−H stretching signal, which can be ascribed to the presence of dangling OH groups.[5−11] This feature not only is observed at the liquid/vapor interface of water but also is clearly detectable in infrared spectra of ice surfaces[12] at temperatures of the order of ∼170 K. The consideration of isotopic mixtures opens interesting possibilities for local concentration fluctuations at the interface, beyond straightforward estimations based on the global stoichiometry of the mixture. At present, there is large body of experimental[13−15] and theoretical[16−18] work that confirm the preference of H atoms at dangling positions in mixtures that combine H_2O, D_2O, and HOD.

From a theoretical perspective, the correct interpretation of the latter enhancement requires a quantum treatment. Recent path integral molecular dynamics simulations experiments have shown that the temperature dependence of the liquid/vapor fractionation in H_2O/D_2O mixtures can be traced back to differences in the anisotropy of the spatial localization of the nuclei which, in turn, are promoted by the local inter- and intramolecular force fields.[16] Similar effects have also been invoked in interpretations of the stabilization of the light isotope on dangling positions at the water surface.[17]

The consideration of nano- to mesoscopic aqueous clusters represents a new scenario in which the latter features should also be observed. Note that these aggregates are normally generated from adiabatic expansions at temperatures as low as ∼100 K.[19−22] Under these thermal conditions, quantum nuclear effects should necessarily manifest in a more clear fashion. Moreover, the fact that a sizable fraction of the cluster constituents are found at the surface should enhance detection of these segregation effects via, for example, direct spectroscopic measurements.[23] In a related context, isotopic substitution is an important tool to unravel the characteristics of tunneling splitting in aqueous clusters, which can be detected by far-IR, terahertz laser spectroscopy.[24,25] In what follows, we will present results from computer simulations that shed light on the characteristics of the relative thermodynamic stability of H and D atoms at dangling positions in solid-like water nanoclusters, along with an analysis of the temperature dependent modifications anticipated in the intensity of the IR spectra.

We examine equilibrium and dynamical characteristics of solid-like, mixed clusters that combine H_2O as a major component and HOD at much lower concentrations. By solid-like structures, we refer to clusters that exhibit fluctuations in the intermolecular distances much smaller than the corresponding average values and dynamical modes involving exclusively small amplitude vibrations. Considering the magnitude of the equilibrium constant for the $H_2O + D_2O \leftrightarrow 2$ HOD interconversion,[26] $K_{eq} \sim 3.5-3.8$, the presence of

Received: May 23, 2014
Accepted: June 19, 2014

D_2O in such a dilute concentration regime can be safely discarded.

Our description is based on the ring polymer molecular dynamics (RPMD) scheme developed by Manolopoulos et al.[27] For equilibrium properties, the procedure yields similar predictions to the ones obtained by implementing standard path integral molecular dynamics techniques.[28] On the other hand, the method introduces an ad-hoc ansatz that leads to reasonable estimates for quantum time correlation functions. Following our recent cluster analysis,[29] interparticle interactions were modeled using the flexible, nonharmonic, q-TIP4P/F Hamiltonian.[30] Previous studies have pointed out the importance of incorporating anharmonic intramolecular interactions in order to reproduce experimental isotopic liquid/vapor partition equilibrium constants for water.[16] Additional information concerning the basic elements of the RPMD scheme and its technical implementation can be found in the Supporting Information.

Two different cluster sizes were analyzed: the water octamer and a larger aggregate comprised of $N_w = 50$ molecules. The former cluster represents the smallest moiety in which stable states at low temperatures exhibit three-dimensional, cubic-like structures. This symmetry also allows for a clear identification of different hydrogen-bonding connectivity patterns. More specifically, water molecules at the cube vertices exhibit alternation of double-donor-single-acceptor (DDSA) and single-donor-double-acceptor (SDDA) characters (see Figure 1). These characteristics have been clearly identified via experimental IR-signals.[31] On the other hand, $N_w = 50$ clusters below their melting point exhibit roughly spherical structures in which one can distinguish between a bulk-like, inner domain and an external surface shell.

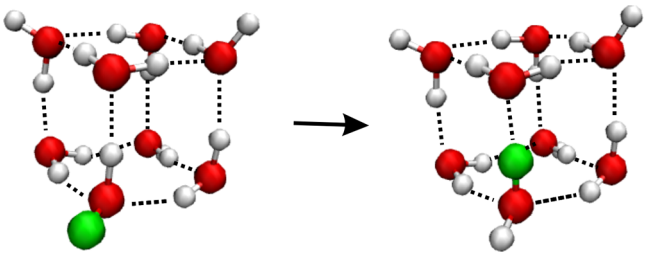

Figure 1. H ↔ D interchange shown in eq 1. For clarity, the D atom in the front SDDA molecule is rendered in green.

The starting point of our analysis involves the consideration of the mixed $[HOD][H_2O]_7$ octamer, in which an HOD molecule is located at one of the SDDA vertices, exhibiting dangling D^d- and connecting H^c-atoms. From this initial arrangement, we analyze the following model interconversion process (see Figure 1)

$$[H_2O]_7H^cOD^d \rightarrow [H_2O]_7H^dOD^c \tag{1}$$

The free energy difference, ΔA, associated with the transformation in eq 1 can be estimated in a straightforward fashion by resorting to standard thermodynamic integration schemes,[32] that is

$$\Delta A = \int_0^1 \left\langle \frac{\partial A(\lambda)}{\partial \lambda} \right\rangle_\lambda \mathrm{d}\lambda \tag{2}$$

In the previous equation, the parameter λ gauges the reversible modifications of the atomic masses of the tagged HOD molecule and $\langle \cdots \rangle_\lambda$ represents a canonical ensemble average taken with atomic masses set at $\{m_i(\lambda)\}$.

Using the virial estimate of the quantum kinetic energy, the integrand of the previous equation can be evaluated as

$$\left\langle \frac{\partial A(\lambda)}{\partial \lambda} \right\rangle_\lambda = -\sum_i \frac{1}{m_i(\lambda)} \frac{\partial m_i(\lambda)}{\partial \lambda} \times \left[\frac{3}{2\beta} + \left\langle \frac{1}{2P} \sum_{j=1}^{P} (\mathbf{r}_i^{(j)} - \mathbf{r}_i^C) \cdot \nabla_{\mathbf{r}_i^{(j)}} V \right\rangle_\lambda \right] \tag{3}$$

where $\mathbf{r}_i^{(j)}$ denotes the coordinate of the ith particle at the imaginary time-slice j, P stands for the number of beads in the isomorphic polymers, $\mathbf{r}_i^C$ is the position of the polymer centroid associated with the ith particle and V represents the potential energy of the system. In this particular case, the integral shown in eq 2 was evaluated following a linear path, namely

$$m_H(\lambda) = m_p(1 + \lambda)$$
$$m_D(\lambda) = m_p(2 - \lambda) \tag{4}$$

where m_p represents the proton mass. Combining eqs 3 and 4, the final expression for the integrand is

$$\left\langle \frac{\partial A(\lambda)}{\partial \lambda} \right\rangle_\lambda = \frac{\langle T_D \rangle_\lambda}{2 - \lambda} - \frac{\langle T_H \rangle_\lambda}{1 + \lambda} \tag{5}$$

where T_i corresponds to the quantum kinetic energy of the ith nucleus.

In Figure 2, we present results for cumulative integrals of the type

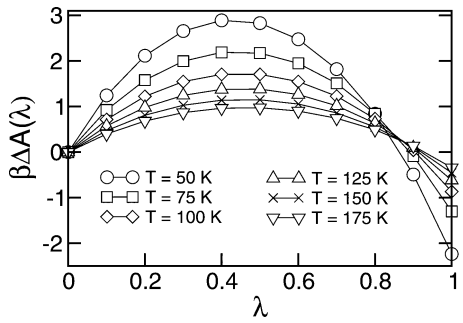

Figure 2. Cumulative integrals for the free energy associated with the isotopic exchange shown in eq 1 at different temperatures.

$$\Delta A(\lambda) = \int_0^\lambda \left\langle \frac{\partial A(\lambda')}{\partial \lambda'} \right\rangle_{\lambda'} \mathrm{d}\lambda' \tag{6}$$

at different temperatures. At a first glance, the plots differ considerably from the symmetric profiles one would obtain assuming a classical description. Moreover, the values on the right-hand vertical axis, and displayed more vividly in Figure 3, reveal a clear stabilization of the H^dOD^c intermolecular connectivity over the H^cOD^d one. As expected, isotope effects become more marked at lower temperatures, reaching $\Delta A \sim -2k_BT$ at $T = 50$ K. The latter difference should be compared to the marginal stabilization reported in ref 17 at the water/air interface at ambient conditions, $\Delta A \sim -0.02k_BT$.

Several arguments can be invoked to rationalize these observations. For example, Ceriotti et al.[33] have undertaken a

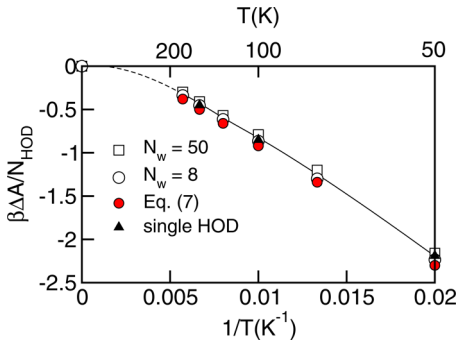

Figure 3. Temperature dependence of the free energy difference associated with isotopic exchange in water clusters. The results are normalized by the number of HOD molecules. The dashed line is an aid to the eye indicating extrapolation to the classical high temperature limit.

detailed examination of the mass dependence of the average quantum kinetic energy operator and found that, for harmonic-like systems, one anticipates $\langle T_i \rangle \propto m_i^{-1/2}$. Assuming that this hypothesis remains valid in the present context, the integral in eq 2 could be approximated by[17]

$$\Delta A \sim 2[1 - (m_H/m_D)^{1/2}](\langle T_{H^d} \rangle - \langle T_{H^c} \rangle) \tag{7}$$

Note that the expression in eq 7 only depends on the difference between the kinetic energies of the light isotope at dangling and connective positions.

Estimates for ΔA at three different temperatures obtained from the approximation in eq 7 are shown in Figure 3 as colored circles. One can see that the quality of Ceriotti et al.'s approximation is remarkably good. Interestingly, the latter feature can be further exploited to account for the observed stabilization in terms of the corresponding spatial extents of the H atoms. Note that basic quantum arguments establish that the average quantum kinetic energy should go hand in hand with the extent of the localization of the individual quantum particles. In a recent analysis,[29] we showed that H^d atoms exhibit more marked spatial delocalization than H^c atoms. Expressed in terms of their corresponding correlation lengths, $\mathcal{R}_i$, where

$$\mathcal{R}_i^2 = \frac{1}{P}\sum_{j=1}^{P} \langle |\mathbf{r}_{H_i}^{(j+P/2)} - \mathbf{r}_{H_i}^{(j)}|^2 \rangle \tag{8}$$

at $T \sim 50$ K polymer sizes associated with dangling and connective atoms in SDDA molecules differ by a factor of $\mathcal{R}_{H^d}/\mathcal{R}_{H^c} \sim 1.5$. As such, we can conclude that the combined effects from intra- and intermolecular interactions not only control the magnitude of the resulting sizes of the isomorphic polymers, but are responsible for the stabilization of the light isotopes at dangling positions as well. We remark that more detailed analyses based on projections of the kinetic energy operator along intramolecular bonds leads to equivalent conclusions.[16,17]

The analysis of larger, that is, $N_w = 50$, aggregates also yields interesting conclusions. In this case, the initial conditions for the RPMD simulations were obtained by first implementing a standard replica-exchange scheme.[34−36] Additional details concerning this procedure are provided as Supporting Information. With this procedure, the vast majority of the solid-like cluster configurations obtained were found to be reasonably well described in terms of quasispherical moieties, exhibiting ∼10−15 dangling atoms, randomly distributed at the external surface.

Three model isotope exchange processes were analyzed. The first one corresponds to simultaneous H-to-D exchanges in all SDDA molecules lying at the cluster surface. Interestingly, within the uncertainties of our simulation experiments, the results for the normalized ΔA displayed in Figure 3 (open squares) are practically identical to those obtained for the water octamer process shown in eq 1. The second experiment consists of several single molecule H−D exchange calculations on randomly selected individual HOD molecules exhibiting a dangling site. For all practical purposes, these new results (shown as black triangles) coincide with the previous sets, suggesting that the total free energy difference is remarkably additive. To complete our thermodynamic analysis, we examined the following model transformation at $T = 150$ K, namely

$$H^dOD^c + H_2O_{blk} \rightarrow H^cOH^d + HOD_{blk} \tag{9}$$

where the subscript blk indicates a molecule located in the central, bulk-like region of the cluster. For this case, the associated free energy difference was found to be $\beta\Delta A = -0.43 \pm 0.03$, a value that compares favorably with the free energy associated with eq 1. As such, the values of ΔA do not seem affected by the diversity of solvation environments examined in this study, a fact that supports a conclusion that the present results should remain valid for a wide range of temperatures, cluster sizes, and relative concentrations.

The picture that emerges from this set of results would then suggest that dangling ↔ connective isotope exchanges would not depend on the location of the connective species. Provided the local concentrations of H_2O and HOD in the "bulk-like" region and at the cluster surface do not differ substantially, the isotope stabilization of the light species at dangling positions can be cast in terms of a more simplified atomic interchange process, namely

$$H^c + D^d \rightarrow H^d + D^c \tag{10}$$

where the superscript c stands for connective atoms, independently of their locations.

Furthermore, one may also speculate on whether the magnitude of the isotopic stabilization could be reported experimentally by significant modifications of spectroscopic signals that, in turn, could be interpreted to infer the thermal characteristics of the clusters. In Figure 4, we present results of the Fourier transform of the time correlation function of the second derivative of the total dipole moment of different clusters, namely

$$\hat{C}(\omega) = \int_0^\infty \langle \dot{\mu}(t)\cdot\dot{\mu}(0)\rangle \cos(\omega t)\mathrm{d}t \tag{11}$$

We remark that, within the RPMD approximation, $\hat{C}(\omega)$ is proportional to the intensity of the IR spectrum of the clusters. Additional information is provided as Supporting Information.

In the top panel of Figure 4, we display results for the stretching band of four different water octamers at $T = 50$ K. The corresponding profile for pure H_2O represents an appropriate reference (solid line). The overall line shape presents four peaks:[29,31] two central ones corresponding to symmetric and asymmetric modes of DDSA molecules and two lateral peaks involving stretching motions localized in SDDA molecules. The replacement of an H_2O by an HDO at a DDSA vertex introduces a new decoupled signal at lower frequencies,

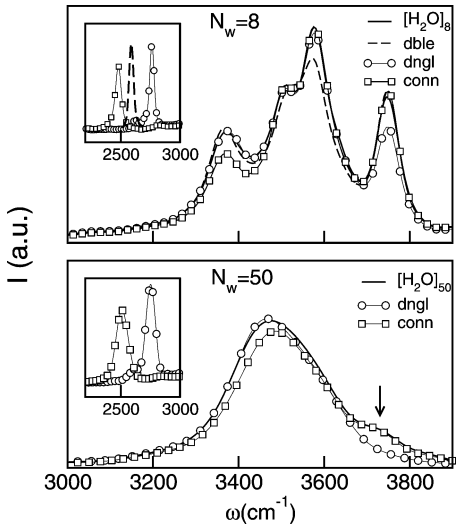

Figure 4. Top panel: IR-spectra of pure and different HOD substituted water octamers (see text) at T = 50 K. Bottom panel: Same as above for N_w = 50 clusters. The arrow indicates the high frequency shoulder corresponding to H^d atoms. Pure light water (solid line); H^cOD^c (dashed lines); D^dOH^c (open circles); D^cOH^d (open squares).

$\omega \sim 2600$ cm^{-1}, associated with O−D stretching motions and a consequent reduction of the high frequency peak in the original central band at $\omega \sim 3580$ cm^{-1} (dashed line). Conversely, if the $H_2O \rightarrow$ HOD substitution is carried out at a SDDA position, the original low frequency peak exhibits a frequency shift and the modifications in the original H-band move to the lateral sub-bands. Clearly, the presence of an $H^cOD^d(H^dOD^d)$ arrangement promotes a blue(red) shift of the O−D signal and a reduction of the dangling-H (connective-H) signal intensity at $\omega \sim 3750$ cm^{-1}($\omega \sim 3370$ cm^{-1}). Interestingly, a more careful analysis of the modifications in the amplitudes of the different peaks are roughly those predicted by the simple consideration of the 4-to-3 reduction in the number of H_2O molecules at SSDA or DDSA positions.

The profiles in the bottom panel of Figure 4 correspond to IR-spectra of N_w = 50 clusters at T = 50 K. The stretching band for the pure H_2O aggregate looks much broader and practically structureless, except for a high frequency shoulder located at $\omega \sim 3730$ cm^{-1}; this corresponds to stretching modes associated with H^d atoms (solid line). For the sake of comparison, we also show lineshapes for two limiting situations in which all dangling positions are occupied by D^d or H^d atoms of HOD molecules. As expected, these substitutions give rise to new decoupled O−D signals at lower frequencies whereas the presence of D^d atoms leads to the disappearance of the above-mentioned high-frequency shoulder. Note that the presence of D^c does not affect the overall line shape in a transparent fashion.

We can then conclude that the intensity of the high frequency shoulder would be indicative of the actual concentration of H^d-atoms which, according to our previous thermodynamic analysis, would depend on the global stoichiometry of the particular mixture considered and on the prevailing temperature, as well. From eq 10, the quantum-isotope-induced enhancement of the peak intensity $I(x_H,T)$ at a given global mole fraction of H atoms x_H can written as

$$\frac{I(x_H, T)}{x_H I(x_H = 1, T)} = \frac{1}{x_H + e^{\beta\Delta A}(1 - x_H)} \tag{12}$$

where the product $x_H I(x_H = 1,T)$ represents the expected peak intensity based on the sole consideration of the overall stoichiometry of the mixture. To provide numerical estimates of the magnitude of the expected changes, for an x_H = 0.8 mixed cluster, the quantum enhancement should be of the order of ∼20%(∼10%) at T = 50 K (T = 150 K).

The results presented in this paper corroborate the thermodynamic stability of light isotopes at dangling positions located at the surface of isotopically mixed water clusters that combine H_2O and HOD species. For temperatures of below, say, 100 K, the free energy is similar to classical thermal energies. The analysis of the water octamer revealed that the origins of the stability are to be found in differences in the spatial extent of protons that are controlled by the local characteristics of both intermolecular and intramolecular interactions. We have also established that the relative prevalence of H atoms can be clearly detected by the concomitant modifications in the magnitude of the high frequency shoulder of the stretching band of the cluster and that this, in turn, would provide an indirect route to assess the thermal characteristics of the clusters. As a natural extension of the present results, we are currently investigating the potential for this kind of spectroscopic approach to distinguish bulk from surface solvation states of probes in aqueous nanoclusters.

■ ASSOCIATED CONTENT

Supporting Information

Additional details concerning the technical implementation of the simulations is provided. This material is available free of charge via the Internet at http://pubs.acs.org.

■ AUTHOR INFORMATION

Corresponding Author

*D. Laria. E-mail: dhlaria@cnea.gov.ar.

Notes

The authors declare no competing financial interest.

■ ACKNOWLEDGMENTS

D.L. is a staff member of CONICET-Argentina. P.J.R. acknowledges the support of the U.S. National Science Foundation (CHE-1362381). Additional support from the R. A. Welch Foundation (F-0019) is gratefully acknowledged.

■ REFERENCES

(1) Richmond, G. L. Molecular Bonding and Interactions at Aqueous Surfaces as Probed by Vibrational Sum Frequency Spectroscopy. *Chem. Rev.* **2002**, *102*, 2693−2724.

(2) Gopalakrishnan, S.; Liu, D. F.; Allen, H. C.; Kuo, M.; Shultz, M. J. Vibrational Spectroscopic Studies of Aqueous Interfaces: Salts, Acids, Bases, and Nanodrops. *Chem. Rev.* **2006**, *106*, 1155−1175.

(3) Shen, Y. R.; Ostroverkhov, V. Sum-Frequency Vibrational Spectroscopy on Water Interfaces: Polar Orientaion of Water Molecules at Interfaces. *Chem. Rev.* **2006**, *106*, 1140−1154.

(4) McGuire, J.; Shen, Y. Ultrafast Vibrational Dynamics at Water Interfaces. *Science* **2006**, *313*, 1945−1948.

(5) Du, Q.; Superfine, R.; Freysz, E.; Shen, Y. R. Vibrational Spectroscopy of Water at the Vapor/Water Interface. *Phys. Rev. Lett.* **1993**, *70*, 2313.

(6) Gragson, D. E.; Richmond, G. L. Investigations of the Structure and Hydrogen Bonding of Water Molecules at Liquid Surfaces by Vibrational Sum Frequency Spectroscopy. *J. Phys. Chem. B* **1998**, *102*, 3847−3861.

(7) Shultz, M. J.; Baldelli, S.; Schnitzer, C.; Simonelli, D. Aqueous Solutions/Air Interfaces Probed with Sum Frequency Generation Spectroscopy. *J. Phys. Chem. B* **2002**, *106*, 5313−5324.
(8) Sovago, M.; Campen, R. K.; Wurpel, G. W.; Muller, M.; Bakker, H. J.; Bonn, M. Vibrational Response of Hydrogen-Bonded Interfacial Water is Dominated by Intramolecular Coupling. *Phys. Rev. Lett.* **2008**, *100*, 173901.
(9) Raymond, E. A.; Tarbuck, T. L.; Brown, M. G.; Richmond, G. L. Hydrogen-Bonding Interactions at the Water/Vapor Interface Investigated by Vibrational Sum-Frequency Spectroscopy of HOD/H_2O/D_2O Mixtures and Molecular Dynamics Simulations. *J. Phys. Chem. B* **2003**, *107*, 546−556.
(10) Raymond, E. A.; Tarbuck, T. L.; Richmond, G. L. Isotopic Dilution Studies of the Vapor/Water Interface as Investigated by Vibrational Sum-Frequency Spectroscopy. *J. Phys. Chem. B* **2002**, *106*, 2817−2820.
(11) Walker, D. S.; Richmond, G. L. Understanding the Effects of Hydrogen Bonding at the Vapor/Water Interface: Vibrational Sum Frequency Spectroscopy of H_2O/HOD/D_2O Mixtures Studied Using Molecular Dynamics Simulations. *J. Phys. Chem. C* **2007**, *111*, 8321−8330.
(12) Wei, X.; Miranda, P. B.; Shen, Y. R. Surface Vibrational Spectroscopic Study of Surface Melting of Ice. *Phys. Rev. Lett.* **2001**, *86*, 1554.
(13) Devlin, J. P. Preferential Deuterium Bonding at the Ice Surface: A Probe of Surface Water Molecule Mobility. *J. Chem. Phys.* **2000**, *112*, 5527.
(14) Rowland, B.; Fisher, M.; Devlin, J. P. Probing Icy Surfaces with the Dangling-OH-mode Absorption: Large Ice Clusters and Microporous Amorphous Ice. *J. Chem. Phys.* **1991**, *95*, 1378.
(15) Devlin, J. P.; Buch, V. Surface of Ice As Viewed from Combined Spectroscopic and Computer Modeling Studies. *J. Phys. Chem.* **1995**, *99*, 16534−16548.
(16) Markland, T. E.; Berne, B. J. Unraveling Quantum Mechanical Effects in Water Using Isotopic Fractionation. *Proc. Natl. Acad. Sci. U. S. A.* **2012**, *109*, 7988−7991.
(17) Liu, J.; Andino, R. S.; Miller, C. M.; Chen, X.; Wilkins, D. M.; Ceriotti, M.; Manolopoulos, D. E. A Surface-Specific Isotope Effect in Mixture of Light and Heavy Water. *J. Phys. Chem. C* **2013**, *117*, 2944−2951.
(18) Nagata, Y.; Pool, R. E.; Backus, E. H. G.; Bonn, M. Nuclear Quantum Effects Affect Bond Orientation of Water at the Water-Vapor Interface. *Phys. Rev. Lett.* **2012**, *109*, 226101.
(19) Ayotte, P.; Johnson, M. A. Electronic Absorption Spectra of Size-Selected Hydrated Electron Clusters: $(H_2O)_n^-$, n = 6−50. *J. Chem. Phys.* **1997**, *106*, 811.
(20) Verlet, J. R.; Bragg, A. E.; Kammrath, A.; Cheshnovsky, O.; Neumark, D. M. Observation of Large Water-Cluster Anions with Surface-Bound Excess Electrons. *Science* **2005**, *307*, 93−96.
(21) Kammrath, A.; Verlet, J. R.; Griffin, G. B.; Neumark, D. M. Photoelectron Spectroscopy of Large $(\mathrm{Water})_n^-$ (n = 50−200) Clusters at 4.7eV. *J. Chem. Phys.* **2006**, *125*, 076101.
(22) Verlet, J. R.; Bragg, A. E.; Kammrath, A.; Cheshnovsky, O.; Neumark, D. M. Comment on Characterization of Excess Electrons in Water-Cluster Anions by Quantum Simulations. *Science* **2005**, *310*, 1769.
(23) Buck, U.; Huisken, F. Infrared Spectroscopy of Size-Selected Water and Methanol Clusters. *Chem. Rev.* **2000**, *100*, 3863−3890.
(24) Richardson, J.; Wales, D.; Althorpe, S. C.; McLaughlin, O.; Shih; Saykally, R. Investigation of Terahertz Vibration−Rotation−Tunneling Spectra for the Water Octamer. *J. Phys. Chem. A* **2013**, *117*, 6960−6966.
(25) Keutsch, F. N.; Saykally, R. J. Water Clusters: Untangling the Mysteries of the Liquid, One Molecule at a Time. *Proc. Natl. Acad. Sci. U. S. A.* **2001**, *98*, 10533−10540.
(26) Hewitt, A. J.; Doss, N.; Zobov, N. F.; Polyansky, O. L.; Tennyson, J. Deutered Water: Partition Functions and Equilibium Constants. *Mon. Not. R. Astron. Soc.* **2005**, *356*, 1123−1126.
(27) Habershon, S.; Manolopoulos, D. E.; Markland, T. E.; Miller, T. F., III Ring-Polymer Molecular Dynamics: Quantum Effects in Chemical Dynamics from Classical Trajectories in an Extended Phase Space. *Annu. Rev. Phys. Chem.* **2013**, *64*, 387−413.
(28) See, for example, Tuckerman, M. E. *Statistical Mechanics: Theory and Molecular Simulation*; Oxford University Press: Oxford, U. K., 2010; Ch. 10.
(29) Videla, P. E.; Rossky, P. J.; Laria, D. Nuclear Quantum Effects on the Structure and the Dynamics of $[H_2O]_8$ at Low Temperatures. *J. Chem. Phys.* **2013**, *139*, 174315.
(30) Habershon, S.; Markland, T. E.; Manolopoulos, D. E. Competing Quantum Effects in the Dynamics of a Flexible Water Model. *J. Chem. Phys.* **2009**, *131*, 024501.
(31) Buck, U.; Ettischer, I.; Melzer, M.; Buch, V.; Sadlej, J. Structure and Spectra of Three-Dimensional $(H_2O)_n$ Clusters, n = 8, 9, 10. *Phys. Rev. Lett.* **1998**, *80*, 2578.
(32) Vanicek, J.; Miller, W. H. Efficient Estimators for Quantum Instanton Evaluation of the Kinetic Isotope Effects: Application to the Intramolecular Hydrogen Transfer in Pentadiene. *J. Chem. Phys.* **2007**, *127*, 114309.
(33) Ceriotti, M.; Markland, D. E. Efficient Methods and Practical Guidelines for Simulating Isotope Effects. *J. Chem. Phys.* **2013**, *138*, 14112.
(34) Sugita, Y.; Okamoto, Y. Replica-Exchange Molecular Dynamics Method for Protein Folding. *Chem. Phys. Lett.* **1999**, *314*, 141.
(35) Zhang, W.; Wu, C. Convergence of Replica Exchange Molecular Dynamics. *J. Chem. Phys.* **2005**, *123*, 154105.
(36) Earl, D. J.; Deem, M. W. Parallel Tempering: Theory, Applications, and New Perspectives. *Phys. Chem. Chem. Phys.* **2005**, *7*, 3910−3916.